ISSN 1674-1056
http://cpb.iphy.ac.cn
http://iopscience.iop.org/cpb
中国物理 B
Chinese Physics
中国物理 Chinese Physics B

Unidirectional plasmonic Bragg reflector based on longitudinally asymmetric nanostructures

Mingsong Chen(陈名松), Lulu Pan(潘璐璐), Yuanfu Lu(鲁远甫), Guangyuan Li(李光元)

Citation: Chin. Phys. B . 2019, 28(7): 074208. **doi:** 10.1088/1674-1056/28/7/074208
Journal homepage: http://cpb.iphy.ac.cn; http://iopscience.iop.org/cpb

What follows is a list of articles you may be interested in

Dynamics of Airy beams in parity-time symmetric optical lattices

Rui-Hong Chen(陈睿弘), Wei-Yi Hong(洪伟毅)
Chin. Phys. B . 2019, 28(5): 054202. **doi:** 10.1088/1674-1056/28/5/054202

Loss induced negative refraction and super-prism effect at highly absorptive interface

Jian Wu(吴坚), Tao Wang(王涛), Tianyue Hou(侯天悦), Xuefen Kan(阚雪芬), Cheng Yin(殷澄), Pu Zhou(周朴), Zhuangqi Cao(曹庄琪)
Chin. Phys. B . 2019, 28(5): 054201. **doi:** 10.1088/1674-1056/28/5/054201

Reflected and transmitted powers of arbitrarily polarized plane waves at interface between chiral and achiral media

Yan-Feng Lu(路彦峰), Yi-Ping Han(韩一平)
Chin. Phys. B . 2019, 28(2): 024202. **doi:** 10.1088/1674-1056/28/2/024202

Propagation characteristics of oblique incidence terahertz wave through non-uniform plasma

Antao Chen(陈安涛), Haoyu Sun(孙浩宇), Yiping Han(韩一平), Jiajie Wang(汪加洁), Zhiwei Cui(崔志伟)
Chin. Phys. B . 2019, 28(1): 014201. **doi:** 10.1088/1674-1056/28/1/014201

Generation of Mathieu beams using angular pupil modulation

Zhijun Ren(任志君), Jinping He(何晋平), Yile Shi(施逸乐)
Chin. Phys. B . 2018, 27(12): 124201. **doi:** 10.1088/1674-1056/27/12/124201

Unidirectional plasmonic Bragg reflector based on longitudinally asymmetric nanostructures*

Mingsong Chen(陈名松)[1], Lulu Pan(潘璐璐)[1,2], Yuanfu Lu(鲁远甫)[2,†], and Guangyuan Li(李光元)[2,‡]

[1] School of Information and Communication, Guilin University of Electronic Technology, Guilin 541004, China
[2] Shenzhen Institutes of Advanced Technology, Chinese Academy of Sciences, Shenzhen 518055, China

(Received 19 April 2019; revised manuscript received 14 May 2019; published online 25 June 2019)

Plasmonic Bragg reflectors are essential components in plasmonic circuits. Here we propose a novel type of plasmonic Bragg reflector, which has very high reflectance for the right-side incidence and meanwhile has extremely large absorption for the left-side incidence. This device is composed of longitudinally asymmetric nanostructures in a metal–insulator–metal waveguide. In order to efficiently analyze, design, and optimize the reflection and transmission characteristics of the proposed device, we develop a semi-analytic coupled-mode model. Results show that the reflectance extinction ratio between plasmonic modes incident from the right-side and the left-side reaches 11 dB. We expect this device with such striking unidirectional reflection performance can be used as insulators in nanoplasmonic circuits.

Keywords: plasmonic devices, Bragg reflectors, unidirectional reflection, asymmetric nanostructures

PACS: 42.79.Fm, 42.25.Bs, 78.67.–n **DOI:** 10.1088/1674-1056/28/7/074208

1. Introduction

Plasmonics provides an effective platform for concentrating and guiding light beyond the diffraction limit.[1] Among a variety of plasmonic waveguides, the metal–insulator–metal (MIM) waveguide is attractive for highly-integrated on-chip plasmonic circuits because of its extremely strong field confinement.[2–4] To date, a variety of plasmonic devices based on the MIM waveguide platform have been proposed or demonstrated, such as detectors,[5] reflectors,[6,7] electro-optic switches,[8] nonlinear devices,[9] filters, resonators,[10,11] and sensors.[12,13] Among these MIM waveguide-based devices, plasmonic Bragg reflectors have attracted increasing attention in the last decade.[14–23] This is because plasmonic Bragg reflectors allow guiding and steering of plasmonic modes, which are essential components in plasmonic devices and plasmonic circuits.[24] However, the unit nanostructure and thus the whole structure of a plasmonic Bragg reflector have been restricted to be symmetric in the longitudinal direction, i.e., in the propagation direction. As a result, the reflectance for the left-side incident plasmonic mode always equals to that for the right-side one.

In most literatures, the plasmonic Bragg reflector has been analyzed, designed, and optimized using complex theoretical models such as the Rayleigh expansion, or time-consuming numerical methods such as finite difference time domain (FDTD) and finite element method (FEM). Recently, Li *et al.*[17] developed a quantitative theory based on a semi-analytic coupled-mode model for plasmonic Bragg reflectors which can be composed of various nanostructures, and showed that the design and optimization can be greatly simplified by using this model.

Quite recently, devices for asymmetric propagation of electromagnetic waves have been intensively studied. Various approaches distinct from the Faraday effect have been proposed or demonstrated. For example, Fedotov *et al.*[25] reported a polarization sensitive transmission effect asymmetric with respect to the direction of wave propagation based on a planar chiral structure. Shi *et al.*[26] demonstrated the dual-band asymmetric transmission of linearly polarized electromagnetic waves in two opposite directions based on a bilayered chiral metamaterial. Xu *et al.*[27] demonstrated a waveguide with asymmetric propagation of light based on a gradient index metamaterial.

In this work, we propose a novel type of plasmonic Bragg reflector which has asymmetric reflection with respect to the direction of light and is composed of periodic nanostructures that have longitudinally asymmetric geometry in a MIM waveguide. A semi-analytic coupled-mode model will be developed to analyze, design, and optimize the structure, which greatly reduces the calculation cost and the simulation time. After careful design, a very high reflectance extinction ratio up to 11 dB between plasmonic modes incident from the right and the left ports can be achieved. We will show that the plasmonic mode from one port will be efficiently reflected, whereas from

*Project supported by the Shenzhen Research Foundation, China (Grant Nos. JCYJ20160608153308846, JSGG20170822093953679, and JCYJ20180507182444250), the National Key Research and Development Program of China (Grant No. 2017YFC0803506), the National Natural Science Foundation of China (Grant Nos. 61261033 and 61162007), and the Youth Innovation Promotion Association of Chinese Academy of Sciences (Grant No. 20160320).

†Corresponding author. E-mail: yf.lu@siat.ac.cn
‡Corresponding author. E-mail: gy.li@siat.ac.cn

© 2019 Chinese Physical Society and IOP Publishing Ltd

the other port will be almost totally absorbed. This makes the proposed device a unidirectional reflector and absorber at the same time.

2. Results and discussion

2.1. Theory

Figure 1 illustrates the proposed unidirectional plasmonic Bragg reflector, which is composed of several periodic triangle-shaped nanostructures in a MIM waveguide. The unit nanostructure has width w, height h, and period p in a gold–silica–gold waveguide. The width of the input and output MIM waveguides is set to be D_0 so that the plasmonic waveguide is of single mode.

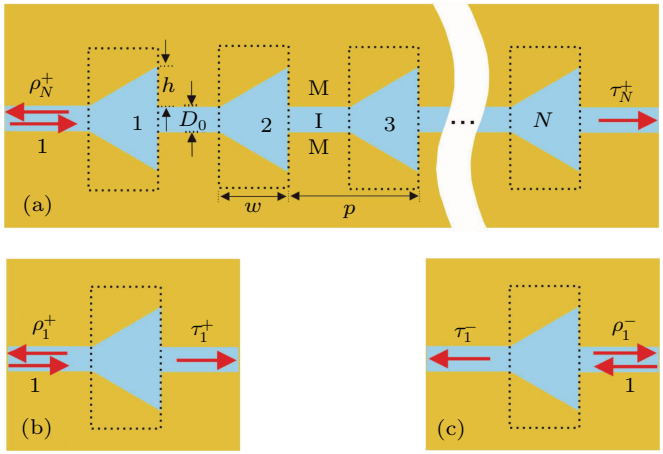


Fig. 1. (a) Schematic of the proposed unidirectional plasmonic Bragg reflector. It is composed of N periodic triangle-shaped nanostructures with period p, width w, and height h. The input and output MIM waveguides have a width of D_0. $\rho_N^{\pm}$ and $\tau_N^{\pm}$ are the reflectance and transmittance coefficients with "+" for the left-side incidence (right-going) and "−" for the right-side incidence (left-going). Each nanostructure is treated as a "black box" (indicated by a dashed box). (b) and (c) The reflectance and transmittance coefficients $\rho_1^{\pm}$ and $\tau_1^{\pm}$ of a single nanostructure (the black box).

In order to efficiently analyze, design, and optimize the proposed structure, we develop a coupled-mode model. Following Ref. [17], we can obtain recursive equations

$$\rho_N^{\pm} = \rho_1^{\pm} + \rho_{N-1}^{\pm} \frac{\tau_1^2 u^2}{1 - \rho_{N-1}^{\pm} \rho_1^{\mp} u^2}, \tag{1}$$

$$\tau_N = \tau_N^{\pm} = \frac{\tau_{N-1} \tau_1 u}{1 - \rho_{N-1}^{+} \rho_1^{-} u^2}, \tag{2}$$

where $\rho_N^{\pm}$ and $\tau_N^{\pm}$ denote the reflectance and transmittance coefficients of the plasmonic Bragg reflector composed of N periodic nanostructures, and the superscripts "+" and "−" are for the right-going and the left-going plasmonic waveguide modes, respectively. Thus $\rho_1^{\pm}$ and $\tau_1^{\pm}$ denote the reflectance and transmittance coefficients of a single nanostructure in the MIM waveguide, respectively, as illustrated in Figs. 1(b) and 1(c). Here $u = \exp[\mathrm{i}k_0 n_{\mathrm{eff}}(p-w)]$, where n_{eff} is the complex effective refractive index of the plasmonic MIM waveguide mode, and $k_0 = 2\pi/\lambda$ is the wave vector in the vacuum. Note that $\tau_m = \tau_m^+ = \tau_m^-$ is valid for $m = 1, \ldots, N$ according to the principle of optical reversibility. Therefore, the reflectance and the transmittance of the plasmonic Bragg reflector can be calculated using $R^{\pm} = |\rho_N^{\pm}|^2$ and $T = |\tau_N|^2$.

The theoretical model treats the unit nanostructure in the MIM waveguide as a black box. By doing this, the effects of the nanostructure's shape, size, and refractive index profile are embodied in $\rho_1^{\pm}$ and τ_1. This treatment makes the model very versatile for nanostructures of any shape. Equations (1) and (2) bridge the reflectance and the transmittance of N periodic nanostructures to those of a single one. Because the computational cost of these recursive equations is trivial, the computational cost for calculating $\rho_N^{\pm}$ and τ_N with Eqs. (1) and (2) approximately equals to that for calculating $\rho_1^{\pm}$ and τ_1. This will significantly reduce the computational cost if one needs to optimize all the geometric parameters. Specifically, by using purely numerical methods such as FDTD or FEM, a global optimization of the reflection performance requires three nested loops for simultaneously scanning w, h, and p for given N, which is very time-consuming and computational complex if N is very large. In contrast, the developed coupled-mode model needs to scan only w and h for a single nanostruture ($N = 1$), and then the optimization of p is performed using the efficient recursive equations. Therefore, the developed model will make the analysis, design, and optimization of the plasmonic Bragg reflector extremely efficient in terms of both time and computation cost.

2.2. Design and optimization

Using the above developed model, we first calculated $\rho_1^{\pm}$ and τ_1 with the fully vectorial simulations based on aperiodic Fourier modal method (a-FMM).[28,29] With the information of $\rho_1^{\pm}$ and τ_1 as functions of the unit nanostructure's size w and h, we then calculated $R^{\pm}$, T, and $|R^+ - R^-|$ of the SPP-Bragg reflector using the recursive equations, i.e., Eqs. (1) and (2). In this work, all the calculations were performed with $n_{\mathrm{SiO_2}} = 1.45$, $D_0 = 100$ nm, and the frequency-dependent relative permittivities of gold tabulated in Ref. [30].

We performed optimization by varying w, h, and p for $N = 4$. Figure 2 shows the results of R^-, R^+, and $|R^+ - R^-|$ as functions of w and h for the optimized period of $p = 280$ nm. Note that, as we will show later, four periods of triangle-shaped nanostructures can result in saturated reflectance difference between the two incident directions, although more nanostructures introduce negligible additional computational cost. From Fig. 2(c), we find that the optimized nanostructure's size for the maximum reflectance difference between R^- and R^+ is $w = 210$ nm and $h = 150$ nm, corresponding to $\max\{|R^+ - R^-|\} = 0.814$. Figure 2(c) also shows that a large reflectance difference can be achieved only a small range of w and h, indicating that the longitudinal asymmetrical triangle-shape nanostructure should be delicately designed in order to

achieve high performance of unidirectional reflection.

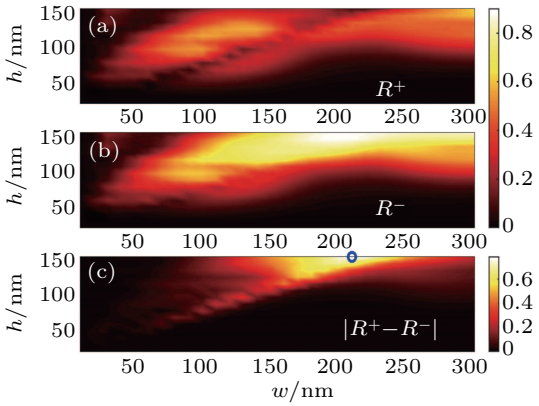


Fig. 2. (a) R^+, (b) R^-, and (c) $|R^+ - R^-|$ as functions of the nanostructure's size w and h. The calculations were performed with $N = 4$, $p = 280$ nm, and $\lambda = 800$ nm. The blue circle in (c) indicates the location of w and h for the maximum value of $|R^+ - R^-| = 0.814$: $w = 210$ nm, $h = 150$ nm.

We investigated the effects of the operation wavelength, the period, and the number of nanostructures on the reflectance and the transmittance of the plasmonic Bragg reflector. Figure 3(a) shows that R^- is always larger than R^+ for wavelengths from the visible to the near infrared, and the maximum reflectance difference locates around $\lambda = 800$ nm, corresponding to $R^- = 0.884$ and $R^+ = 0.07$. Similar to an isolator, we can define reflectance extinction ratio $10\lg(R^-/R^+)$ as a figure of merit for the unidirectional reflection performance. At $\lambda = 800$ nm, the reflectance extinction ratio is as high as 10.97 dB. We also find that over a bandwidth of 50 nm, a reflectance extinction ratio above 10 dB can be achieved. Note that the curve in Fig. 3(a) is not smooth enough since we used 5 nm as the wavelength step.

Figure 3(b) shows that the reflectance versus the nanostructure period exhibits periodic behaviors. For periods of $p = 280$ nm, $p = 500$ nm, and $p = 720$ nm, the reflectance reaches the maximum values. The maximum values slightly decrease as the period increases.

Figure 3(c) shows that, as the number of nanostructures increases, the reflectance for the mode incident from the right port R^- first increases dramatically and soon saturates after $N = 4$, whereas the reflectance for the mode incident from the left port R^+ first slightly increases and also saturates after $N = 4$. Therefore, the reflectance extinction ratio also first increases dramatically and then saturates after $N = 4$. In other words, $N = 4$ can achieve a sufficient reflectance extinction ratio.

Because the transmittance is negligible, this striking reflectance extinction ratio indicates that, if the plasmonic waveguide mode is incident from the right port, most of the power will be reflected back, whereas most power will be absorbed if the mode is incident from the left port. This is better shown by the magnetic field maps of $|H_y|$ in Fig. 4, which were calculated by the a-FMM. It is evident that the reflectance is very weak and the transmittance is negligible when the plasmonic mode impinges from the left side, as shown in Fig. 4(a), and that strong reflection and negligible transmission can be observed for the right-side incidence, as shown in Fig. 4(b).

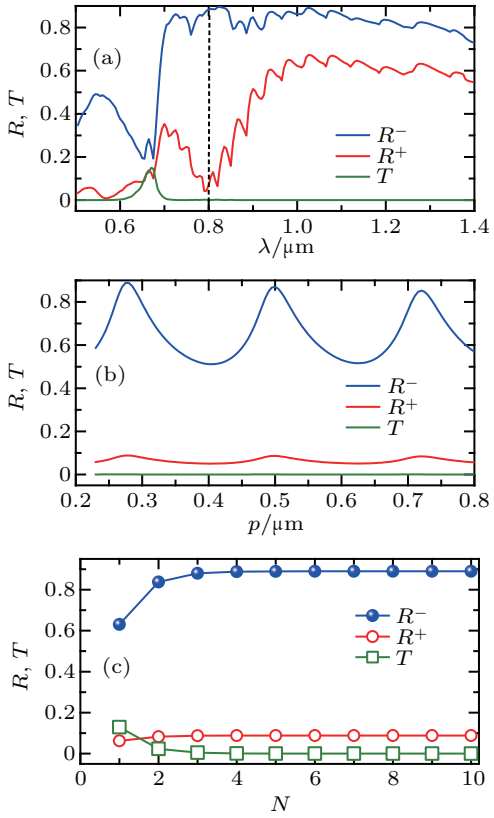


Fig. 3. $R^{\pm}$ and T versus (a) the operating wavelength, (b) the period, and (c) the number of nanostructures. Except for the varying parameters, the calculations are performed with $h = 150$ nm, $w = 210$ nm, $p = 280$ nm, $N = 4$, and $\lambda = 800$ nm.

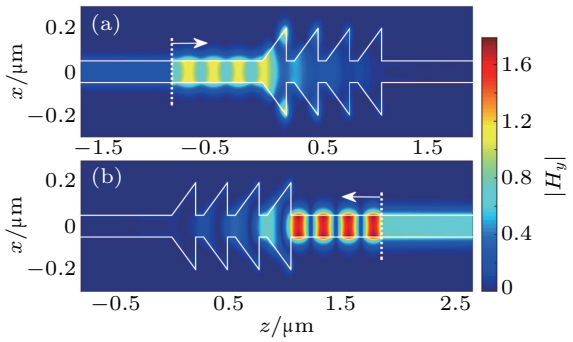


Fig. 4. The field distributions of $|H_y|$ when the plasmonic waveguide modes are incident from (a) the left and (b) the right ports. The central silica core is outline by the white solid-thin lines. The vertical dashed lines indicate the input planes with arrows suggesting the incident directions. The calculations were performed with the same parameters as those in Fig. 3.

In the literature, plasmonic Bragg reflectors composed of symmetric nanostructures in the longitudinal direction always have the same reflection, transmission, and absorption for the left- and right-side incidences. For the proposed device, however, there exists a very large difference in the reflection and absorption between the left- and right-side incidences. We surmise that such striking performance should arise from the

nanostructure's longitudinally asymmetric shape. This speculation can be confirmed by Fig. 2(c), which shows that the higher the nanostructure, the larger the reflectance extinction ratio. This is because a higher nanosctructure indicates more asymmetric in the longitudinal direction. Moreover, figure 4 shows that, for the left-side incidence, the fields are scattered to the wings of the triangle-shaped nanostructures and thus experience more ohmic loss; however, for the right-side incidence, the scattered fields are mainly distributed in the center of the tapered nanostructure.

3. Conclusion

We have proposed a unidirectional plasmonic Bragg reflector composed of a few periodic triangle-shaped nanostructures in the MIM waveguide. A semi-analytic coupled-mode model has been used to efficiently analyze and design this device. Theoretical results showed that the reflectance and absorbance strongly depend on the direction of the incidence. By properly designing the geometrical parameters, we have achieved remarkably large reflectance differences: more than 88% power is reflected for the plasmonic mode incident from the right port, while only 7% power for the incidence from the left port is reflected, corresponding to a reflectance extinction ratio above 10 dB over 50 nm wavelength range. Since this passive device is direction-sensitive and very compact, we expect it will find applications in highly-integrated plasmonic circuits.

References

[1] Gramotnev D K and Bozhevolnyi S I 2010 *Nat. Photon.* **4** 83
[2] Oulton R F, Bartal G, Pile D F P and Zhang X 2008 *New J. Phys.* **10** 105018
[3] Han Z and Bozhevolnyi S I 2013 *Rep. Prog. Phys.* **76** 016402
[4] Fang Y and Sun M 2015 *Light Sci. Appl.* **4** e294
[5] Neutens P, Van Dorpe P, De Vlaminck L L I and Borghs G 2009 *Nat. Photon.* **3** 283
[6] Chen J, Yang J, Chen Z, Fang Y J, Zhan P and Wang Z L 2012 *AIP Adv.* **2** 012145
[7] Zhang Z D, Ma L J, Gao F, Zhang Y J, Tang J, Cao H L, Zhang B Z, Wang J C, Yan S B and Xue C Y 2017 *Chin. Phys. B* **26** 124212
[8] Zhu Y J, Huang X G and Mei X 2012 *Chin. Phys. Lett.* **29** 064214
[9] Nielsen M P, Shi X, Dichtl P, Maier S A and Oulton R F 2017 *Science* **358** 1179
[10] Zhang Z D, Zhao Y N, Lu D, Xiong Z H and Zhang Z Y 2012 *Acta Phys. Sin.* **61** 187301 (in Chinese)
[11] Zhang H Y, Shen D L, Zhang Y P, Yang W J, Yuan C, Liu M, Yin Y H and Wu Z X 2014 *Chin. Phys. B* **23** 097301
[12] Zhu J H, Huang X G and Mei X 2011 *Chin. Phys. Lett.* **28** 054205
[13] Qi Y P, Zhang X W, Zhou P Y, Hu B B and Wang X X 2018 *Acta Phys. Sin.* **67** 197301 (in Chinese)
[14] Hosseini A, Nejati H and Massoud Y 2008 *Opt. Express* **16** 1475
[15] Mu J W and Huang W P 2009 *J. Lightw. Technol.* **27** 436
[16] Liu Y, Liu Y and Kim J 2010 *Opt. Express* **18** 11589
[17] Li G, Cai L, Xiao F, Pei Y and Xu A 2010 *Opt. Express* **18** 10487
[18] Jafarian B, Nozhat N and Granpayeh N 2011 *J. Opt. Soc. Korea* **15** 118
[19] Chen L, Zhang T and Li X 2013 *Chin. Phys. B* **22** 077301
[20] Yun B, Hu G, Zhang R and Cui Y 2014 *Opt. Express* **22** 28662
[21] Tao J, Yu X, Hu B, Dubrovkin A and Wang Q J 2014 *Opt. Lett.* **39** 271
[22] Wang H, Yang J, Wu W, Huang J, Zhang J, Yan P, Chen D and Xiao G 2016 *IEEE Photon. Technol. Lett.* **28** 2467
[23] Wang J, Niu Y, Liu D, Hu Z D, Sang T and Gao S 2018 *Plasmonics* **13** 609
[24] Sorger V J, Oulton R F, Ma R M and Zhang X 2012 *MRS Bull.* **37** 728
[25] Fedotov V A, Mladyonov P L, Prosvirnin S L, Rogacheva A V, Chen Y and Zheludev N I 2006 *Phys. Rev. Lett.* **97** 167401
[26] Shi J, Liu X, Yu S, Lv T, Zhu Z, Ma H F and Cui T J 2013 *Appl. Phys. Lett.* **102** 191905
[27] Xu Y, Gu C, Hou B, Lai Y, Li J and Chen H 2013 *Nat. Commun.* **4** 2561
[28] Moharam M G, Pommet D A and Grann E B 1995 *J. Opt. Soc. Am. A* **12** 1077
[29] Silberstein E, Lalanne P, Hugonin J P and Cao Q 2001 *J. Opt. Soc. Am. A* **18** 2865
[30] Palik E D 1985 *Handbook of Optical Constants of Solids* (New York: Academic)